**DOI:** https://doi.org/10.14525/JJCE.v20i1.05



## **Jordan Journal of Civil Engineering**

Journal homepage: <a href="https://jjce.just.edu.jo">https://jjce.just.edu.jo</a>



# Numerical Investigation of the Performance of Sand Columns in Soft Clay Improvement

LAOUCHE Mohamed 1)\*, BEZIH Kamel<sup>2</sup>), DJENANE Mohamed <sup>2</sup>), KARECH Toufik <sup>3</sup>)

- <sup>1)</sup> LGCE, Laboratory of Civil Engineering and Environment, Department of Civil Engineering and Hydraulics, Faculty of Science and Technology, University Mohamed Seddik ben Yahia, Jijel 18000, Algeria.
  - \*Corresponding Author. E-Mail: mohamed.laouche@univ-jijel.dz
- <sup>2)</sup> LGC-ROI, Laboratory of Civil Engineering Risks and Structures in Interactions, Department of Civil Engineering, Faculty of Technology, University of Batna 2 Mostefa ben Boulaïd-, Batna 05000, Algeria.
- <sup>3)</sup> LRNAT, Laboratory of Natural Risks and Territorial Design, Department of Civil Engineering, Faculty of Technology, University of Batna2 Mostefa ben Boulaïd-, Batna 05000, Algeria.

ARTICLE INFO

ABSTRACT

Article History: Received: 22/5/2025 Accepted: 17/8/2025

This study examines the effects of installing stone columns in soft clay using numerical simulations of small-scale laboratory tests. These tests involve reinforcing Kaolin specimens with sand columns constructed using two techniques: simple replacement without compaction and replacement with compaction. After installation, the specimens were subjected to loading to evaluate their mechanical behavior. A parametric study was conducted to assess the influence of key factors, including area replacement ratio, geogrid confinement, column length, and intensity of compaction stress. The results showed that settlement reduction is proportional to the area replacement ratio, column length, and the stiffness of the geogrid encasement. For a 16% area replacement ratio, the relative settlement decreased from 14.6% to 12.1%, with a corresponding stress concentration ratio of 1.92. When geogrid confinement was applied, settlement was further reduced to 6.9% and stress concentration ratio increased to 15.9. Moreover, columns installed with compaction led to a 20% reduction in the void ratio near the column, lowering the settlement to 9.23%. This reduction was directly related to the intensity of the compaction stress applied. The study highlighted the importance of the column installation method on the behavior of reinforced soils.

*Keywords:* Reinforcement, Sand columns, Settlement, Consolidation, Encasement, Compaction.

## INTRODUCTION

Reinforcement using stone columns is a technique used to improve bearing capacity and reduce foundation settlement in soft soils by accelerating consolidation due to their high permeability. A considerable number of analytical studies have focused on estimating the bearing capacity and settlement characteristics of foundations supported by stone column-improved ground (Greenwood, 1970; Hughes et al., 1976; Aboshi,

1979; Priebe, 1976, 1995; Poorooshasb & Meyerhof, 1996; Balaam et al., 1978; Han & Ye, 2001; Das & Dey 2022; Ghazavi et al., 2024).

Numerical analyses have also played a significant role in evaluating the performance of such systems. Hadri et al. (2021) analyzed the reinforcement of a compressible soil using stone columns through 2D finite-element modeling, applying the equivalent area method. A parametric study highlighted the influence of factors, such as column stiffness, diameter, and spacing.

Whether the column is floating or end-bearing on a rigid layer, bulging remains the primary failure mechanism (Madahy, 2006; Grizi et al., 2022). In soft clays, the effectiveness of stone columns can be considerably reduced due to insufficient lateral confinement, particularly near the upper portion of the column (Hanna et al., 2013; Etezad et al., 2018; Tan et al., 2021). To mitigate this limitation, geo-synthetic encasement has been widely adopted, offering enhanced lateral support and improved load transfer capabilities (Yoo, 2010; Yoo et al., 2009; Gniel & Bouazza, 2009; Cengiz & Guler, 2020; Murugesan & Rajagopal, 2006; El Saied et al., 2022; Borges, 2024).

Floating stone columns have proven to be effective for improving very soft clay soils. Karkush and Jabbar (2019, 2022a, 2022b) demonstrated significant gains in bearing capacity (up to 145%) and reductions in compressibility and excess pore pressure, even without end bearing and with low area replacement ratios. Performance was further enhanced by increasing the number of columns, particularly in quadrilateral arrangements. However, Basack et al. (2016) noted that such conditions may lead to excess pore pressure buildup, partially drained behavior, and clogging at the column-soil interface, compromising drainage efficiency. More recently, Tai et al. (2024) confirmed that floating stone columns significantly reduce settlement and control excess pore pressure, although higher cyclic stress ratios lead to increased stress concentration within the columns. Many researchers have investigated the seismic behavior of stone columns in soft clay. Karkush et al. (2021) showed that floating stone columns improve the seismic performance of soft clay by reducing acceleration, displacement, and velocity. However, Elsiragy (2021) indicated that closely spaced, larger-diameter stone columns improve bearing capacity and reduce settlement. Additionally, geo-textile encasement further enhances performance under seismic loading.

Experimental studies with scaled models also explored factors, like column length and diameter, often using the replacement method removing soft soil and replacing it with granular material (Black et al., 2006, 2007; Sivakumar et al., 2004). The performance of stone columns in soft clay is strongly influenced by installation techniques. Phan (2010) demonstrated that methods involving compaction and/or displacement, such as displacement with compaction and replacement

with compaction, lead to improved soil densification and reduced settlement. Similarly, Laouche et al. (2021), through odometer tests, showed that the installation process significantly alters the surrounding soil's behavior, influencing both settlement and compressibility characteristics. Chandrawanshi et al. (2017) found that greater compaction effort improves the performance of stone columns by reducing settlement.

Advanced numerical methods are used to simulate the effects of stone column installation. Some researchers used full 3D models, while others opted for simpler axisymmetric models that simulate installation by applying radial displacements corresponding to the column diameter (Guetif et al., 2007; Castro & Karstunen, 2010; Ellouze et al., 2017). These studies analyzed he behavior of reinforced soil following stone column installation to evaluate improvements in soft soil properties before final loading. The installation is modeled as an undrained lateral expansion that generates excess pore pressures, increases horizontal stresses, modifies the soil structure, and significantly reduces settlement. Rashwan et al. (2025) compared two stone column installation methods in soft clay: a traditional method and a dynamic one, using finiteelement modeling. Both improve soil bearing capacity and stiffness, but the dynamic method shows greater and more extensive gains. It increases lateral pressure (K > 3.4) and stiffness (×3.2), enhancing stability up to six times the column diameter.

The objective of this study is to evaluate the performance of sand columns installed using two different methods: replacement without compaction (WR-NC) and replacement with compaction (WR-WC). The analysis is conducted through numerical modeling of reduced-scale experimental setups previously carried out by Phan (2010), which aimed to realistically simulate the stone column installation process. Initially, the model is validated by comparing the simulation results with experimental observations, demonstrating strong agreement. A subsequent parametric analysis investigated the effects of key factors, such as the area replacement ratio, column length, geogrid encasement, and compaction stress.

#### LABORATORY EXPERIMENTS

Soil specimens were prepared using industrial

kaolin. This material exhibited a Liquid Limit (LL) of 55% and a Plastic Limit (PL) of 47%. For the construction of sand columns, Loire sand washed and sieved to mimic the characteristics of ballast was selected, with particle sizes ranging from 1.00 mm to 1.25 mm. The experimental program was carried out in three main stages. The first stage involved the preparation of kaolin specimens. The kaolin, initially in the form of dry powder, was first mixed with water and then poured into cylindrical molds with a diameter of 150 mm and a height of 200 mm. Subsequently, the kaolin was consolidated under a vertical pressure of 50 kPa. After consolidation, kaolin specimens with the same diameter and a final height of approximately 130 mm were obtained. The second stage consisted of constructing sand columns at the center of the kaolin specimens, as a reinforcement technique.

Sand columns were installed using two distinct techniques: one with replacement without compaction (WR-NC), and the other with replacement with compaction (WR-WC).

The (WR-NC) method involves creating a borehole in the kaolin specimen, and then introducing sand by simple substitution until the column is fully constructed. The column is built without applying any compaction. The (WR-WC) technique involves creating a borehole, then introducing sand in successive 20-mm layers. Each layer is compacted under a well-defined stress. This process is repeated until the column is fully constructed along its entire height.

After the columns were formed, all specimens were saturated for 24 hours in order to homogenize their degree of saturation. Moreover, the concept of saturation makes it possible to experimentally determine the void ratio from a simple measurement of the water content.

The third stage involved subjecting the kaolin–sand column specimens to loading. First, in order to reestablish the initial stress conditions prior to column installation, a re-consolidation step was carried out under a vertical stress of 50 kPa. Subsequently, a uniform vertical load of 150 kPa was applied to all specimens, as illustrated in Figure 1.

### **Numerical Modeling and Validation**

The geometry of the scaled-down model enables axisymmetric analysis, replicating both the dimensions and boundary conditions applied during laboratory experiments. Regarding mechanical boundary conditions, the lateral sides (left and right) are restricted from horizontal movement, the bottom boundary is fixed in the vertical direction, while the top surface remains free to move vertically.

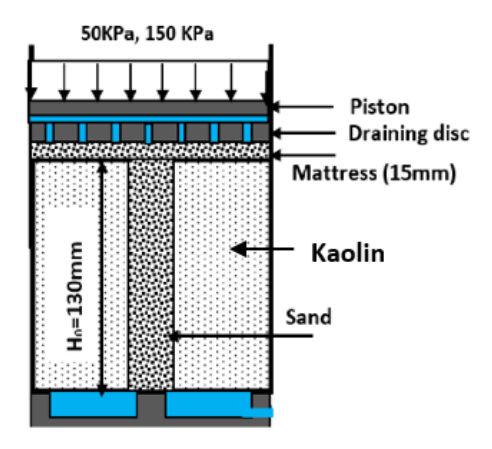


**Figure 1.** A schematic of stress condition on the test sample (Phan, 2010)

For the hydraulic conditions, the lateral boundaries are defined as impermeable, representing the sides of the rigid mold and the model's central axis. Consequently, water flow is permitted exclusively through the top and bottom surfaces of the model.

The vertical load is transmitted through a rigid plate, which ensures an even distribution of settlement across the surface. The plate is defined by the following properties: axial stiffness  $EA=10^5~kN/m$ , bending stiffness  $EI=10^3~kN\cdot m^2/m$ , and a negligible self-weight.

To model material behavior, the Soft Soil Model (SSM) is adopted for kaolin, while the Mohr-Coulomb (MC) model is assigned to both the sand column and the mattress layer. Table 1 provides the geotechnical parameters for the pre-consolidated kaolin, sand column, and mattress materials. The input parameters were obtained from laboratory tests (Phan, 2010). In these tests, the kaolin was subjected to a pre-consolidation stress of 50 kPa, which was subsequently removed, placing the soil in an over-consolidated state prior to the construction of the sand columns. The initial stress state was generated using a Pre-Overburden Pressure (POP) of 50 kPa, an approach available in PLAXIS (Brinkgreve et al., 2011). A POP of 50 kPa reflects prior loading and unloading of the kaolin under the same vertical stress, resulting in an over-consolidated condition.

|                                       | Kaolin | Column/mattress | Column (WR-WC) |
|---------------------------------------|--------|-----------------|----------------|
| Model                                 | SSM    | MC              | MC             |
| $C_c$                                 | 0,38   | -               | -              |
| $C_s$                                 | 0,10   | -               | 1              |
| $\gamma_{sat} (kN/m^3)$               | 16,56  | 19              | 19             |
| $\gamma_{unsat}$ (kN/m <sup>3</sup> ) | 10,56  | 17              | 17             |
| e                                     | 1,52   | 0,5             | 0,5            |
| C (KPa)                               | 1      | 1               | 1              |
| φ ( <sup>0</sup> )                    | 21     | 27              | 27             |
| k (m/s)                               | 4.10-9 | 1.10-4          | 1.10-4         |
| POP (KPa)                             | 50     | -               | -              |
| E                                     | -      | 2.104           | $3.10^4$       |
| v                                     | 0.3    | 0.3             | 0.3            |

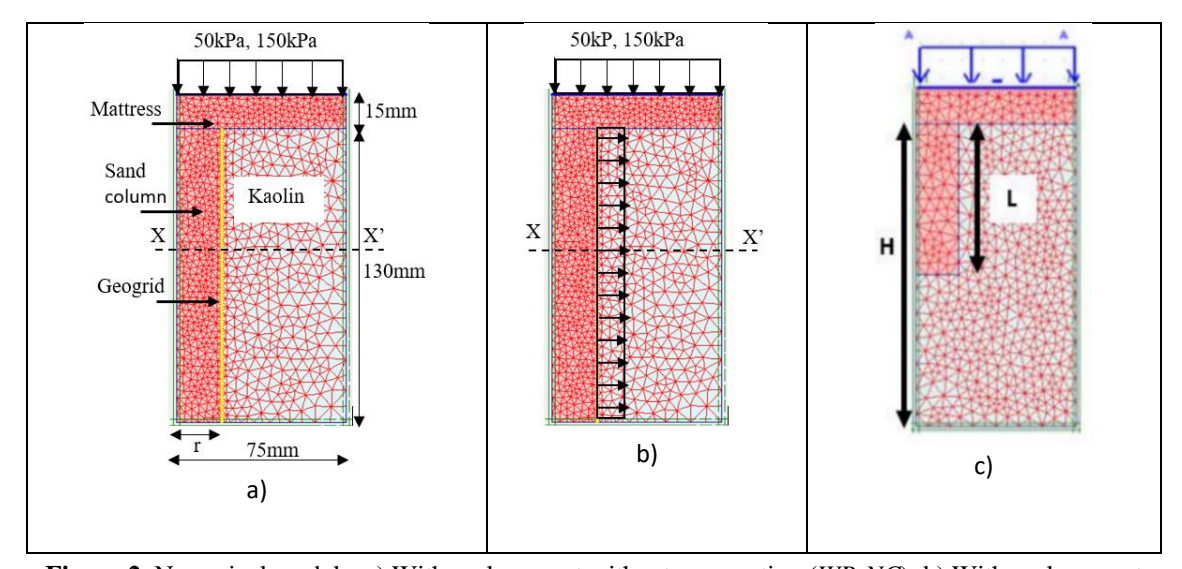
Table 1. Soil parameters

The numerical simulation corresponding to the (WRNC) method, as illustrated in Figure 2a, is carried out through the following sequential steps:

- Creation of a borehole within the pre-consolidated kaolin layer.
- Installation of the sand column within the excavated borehole.
- Placement of a 15 cm-thick sand mattress over the surface.
- Application of a 50 kPa vertical load to re-establish the initial stress conditions, followed by a consolidation phase.
- Imposition of a 150 kPa vertical load to simulate the

loading stage, accompanied by further consolidation. This process continues until the excess pore water pressure throughout the model drops below 1 kPa.

The numerical simulation for the (WR-WC) method, shown in Figure 2b, follows the same procedural steps as the (WR-NC) method, with one key distinction: a uniform radial displacement is applied along the boundary of the sand column to replicate the lateral expansion resulting from compaction during installation (Figure 2b). The numerical strategy adopted to simulate the installation effects of the column is based on the methodology described by Guetif et al. (2007).



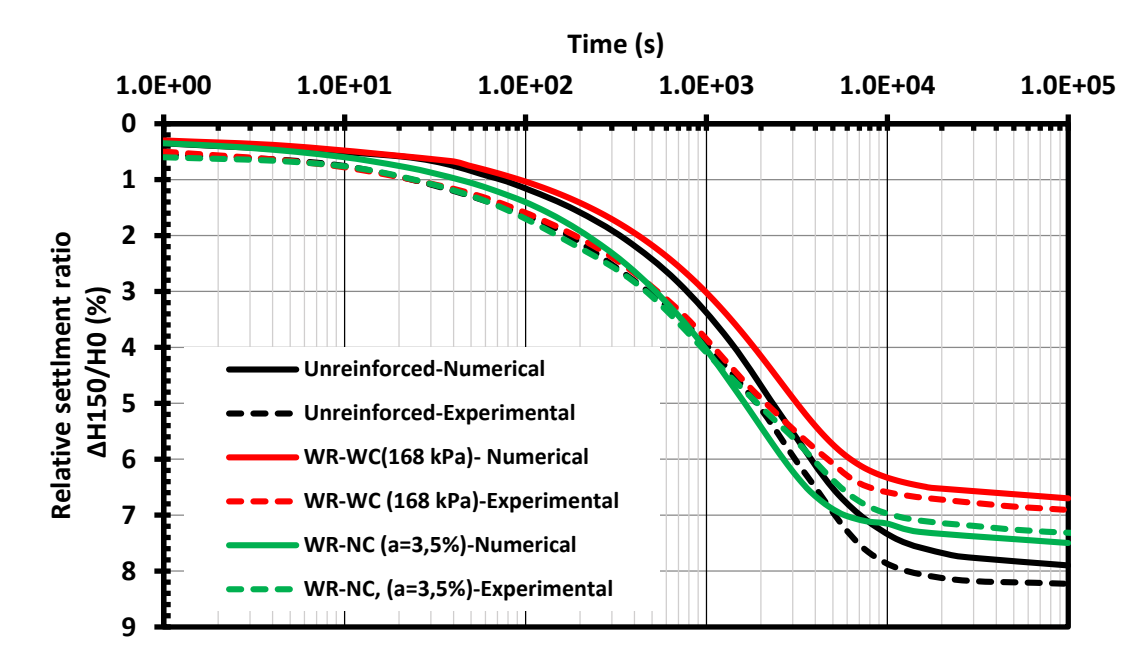
**Figure 2.** Numerical models: a) With replacement without compaction (*WR-NC*); b) With replacement with compaction (*WR-WC*); c) Effect of column length

Figure 3 compares numerical simulations with

experimental data from Phan (2010) regarding the

relative settlement ( $\Delta H_{150}/H_0$ ) over time during the consolidation stage under a constant vertical load of 150 kPa. Here,  $\Delta H_{150}$  denotes the settlement measured under the applied load, and  $H_0$  refers to the initial height of the compressible layer. The analysis includes three scenarios: untreated soil, soil reinforced with a sand column installed with (WR-NC) method at an area

replacement ratio of 3.5%, and soil reinforced with a column installed using the (WR-WC) method under 168 kPa. The loading period was maintained at 10<sup>5</sup> seconds for all cases. Results demonstrated excellent agreement between the numerical predictions and the experimental observations.



**Figure 3.** Comparison between experimental and numerical results for the phase 150 kPa (unreinforced case; WR-NC for a=3,5%; WR-WC for 168kPa)

### RESULTS AND DISCUSSION

# Method with Replacement without Compaction (WR-NC)

In this sub-section, the sand column is constructed without compaction. A parametric analysis is conducted to evaluate the impact of several factors on sand column performance, including the area replacement ratio (a), column length (L) (Figure 2c), and column encasement (Figure 2a). The variable H represents the thickness of the kaolin layer.

#### **Effect of Area Replacement Ratio**

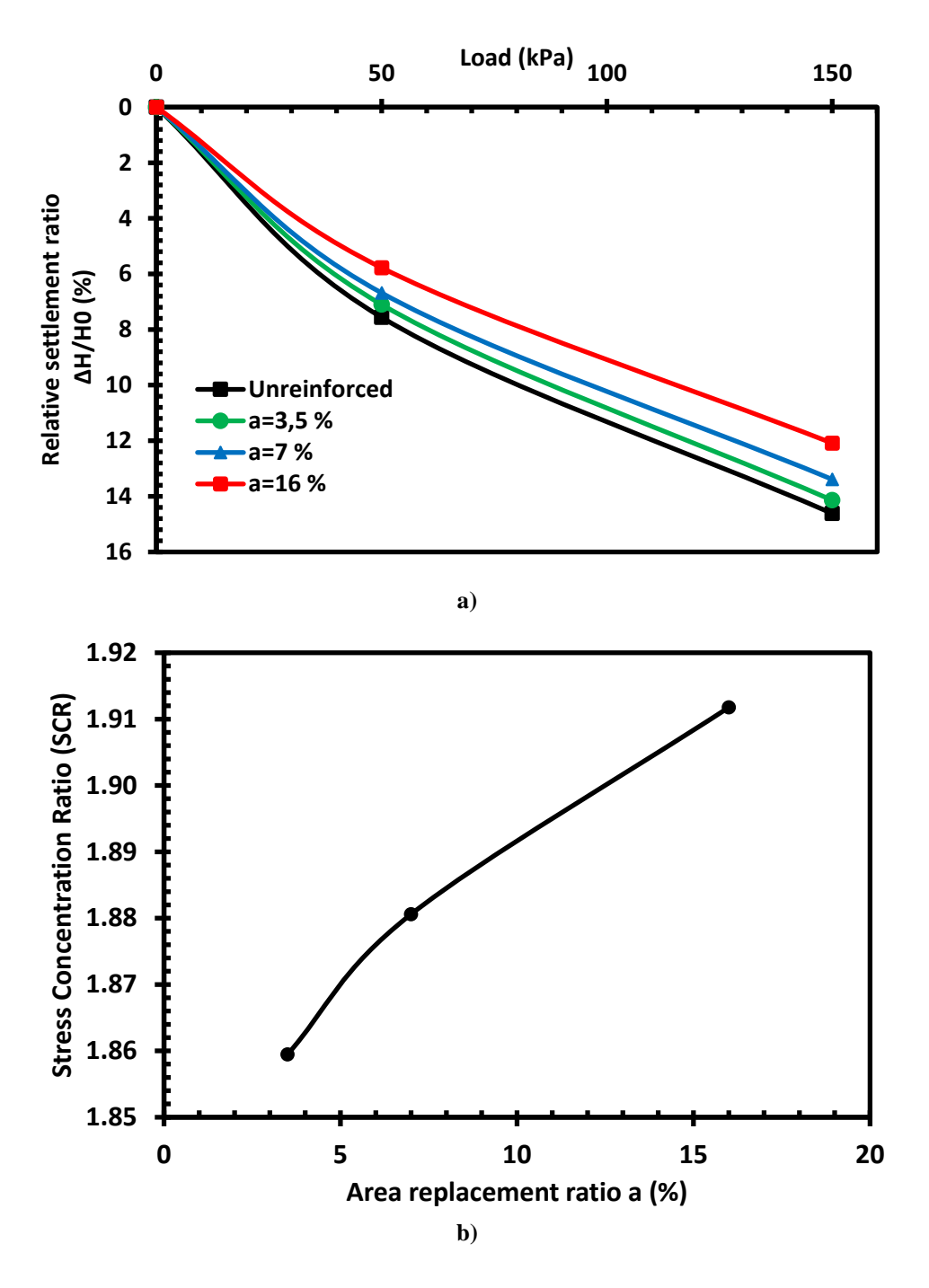
The area replacement ratio is defined as the ratio of the column's cross-sectional area (Ac) to the area of the unit cell (A). Three columns with different diameters (28 mm, 40 mm, and 60 mm) were tested, resulting in area replacement ratios of 3.5%, 7%, and 16%.

Figure 4a illustrates the variation in total settlement  $(\Delta H/H_0)$  with the applied load. The results show a

consistent increase in total settlement with increasing applied loads. Furthermore, settlement is inversely related to the area replacement ratio. The final values of  $(\Delta H/H_0)$  under a load of 150 kPa are 14.1%, 13.4%, and 12.1% for a = 3.5%, a = 7%, and a = 16%, respectively, compared to the unreinforced case, which is 14.4%. These correspond to reductions in total settlement of 3%, 8%, and 17%, respectively. The Stress Concentration Ratio SCR is the ratio between the stress supported by the column and that supported by the soil. The variation of SCR is presented in Figure 4b. It indicates that this factor is proportional to the area replacement ratio. The values are 1.85 for 3.5%, 1.89 for 7%, and 1.92 for 16%, respectively.

The observed decrease in settlement is attributed to the presence of the sand column, which has a higher stiffness than the surrounding soil. This allows stress concentration at the top of the column, reduces stress at ground level, and enhances the stiffness of the soilcolumn system. Figure 4c illustrates the consolidation response of the specimen under an applied load of  $150 \, \text{kPa}$ . The results indicate a reduction in the settlement rate for the reinforced soils. As the area replacement ratio (a) increases, the reduction becomes more significant, reaching 10%, 15%, and 22% for a = 3.5%, a = 7%, and a = 16%, respectively. Moreover, the results show that consolidation is faster in the reinforced

cases. This occurs because the permeability of the columns is higher than that of the clay alone, enabling quicker water drainage through radial flow. The consolidation rate is directly related to the area replacement ratio, since increasing the column diameter reduces the radial drainage distance.



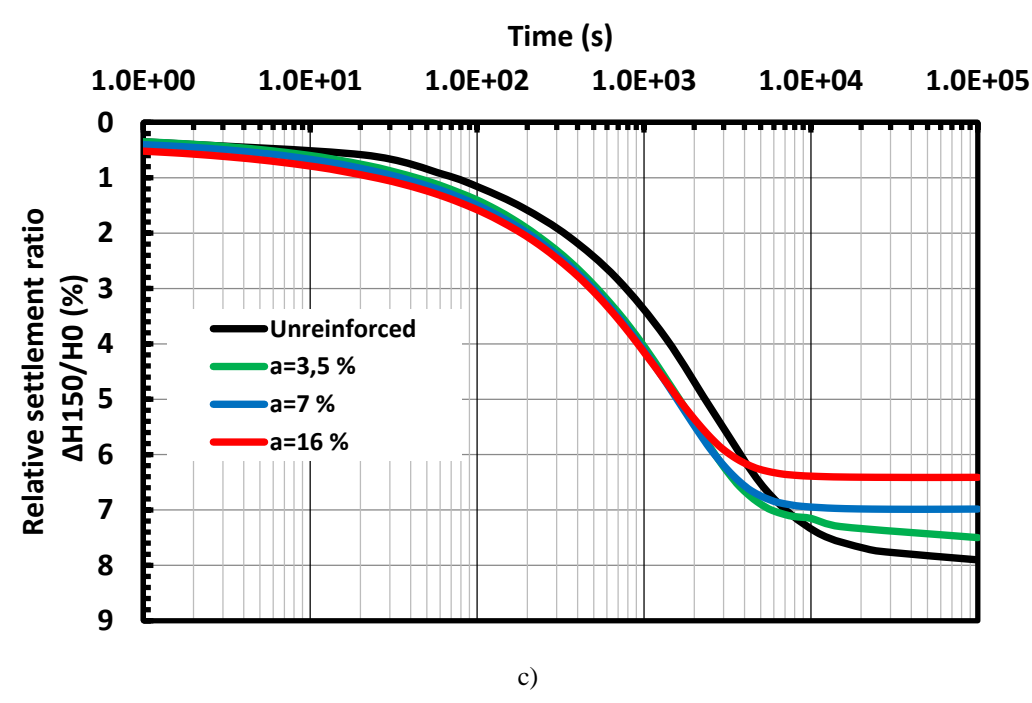


**Figure 4.** Effect of area replacement ratio: a) Total settlement; b) Sress concentration ratio SCR; c) Consolidation (Phase  $\sigma$ =150 kPa)

#### **Effect of Column Length**

This part examines the impact of column length (L) on the performance of the reinforcement (Figure 2c). The study is carried out with a constant area replacement ratio of a=16%, considering three column configurations: two floating columns with L/H ratios of 0.5 and 0.75, and one end-bearing column with an L/H ratio of 1. In this context, H denotes the thickness of the clay layer being reinforced. The results shown in Figure 5a reveal that total settlement increases in direct proportion to the applied load for all column configurations. The final total settlement values ( $\Delta H/H_0$ ) are 13.3% and 12.68% for L/H ratios of 0.5 and 0.75, respectively, compared to 12.1% for L/H = 1. These correspond to settlement reductions of 8.9%, 13.12%, and 17%, respectively.

Among the floating column configurations, the column with L/H = 0.75 exhibits less settlement than the one with L/H = 0.5. As the column length increases, the contact area between the column and the surrounding soil expands, improving the mobilization of lateral friction and reducing settlement. For an L/H ratio of 1, the column is fixed at its base, mobilizing both endbearing resistance and lateral friction along its surface in contact with the soil. This dual mechanism significantly enhances its load-bearing capacity. In contrast, columns

with L/H ratios of 0.5 and 0.75 behave as floating columns, relying primarily on lateral friction for load transfer.

Figure 5b illustrates the variation in settlement  $(\Delta H/H_0)$  for columns with different diameters, corresponding to area replacement ratios of a = 3.5%, 7%, and 16%, in the case of L/H = 0.5. In this configuration, the bearing capacity is primarily governed by friction along the column–soil interface. The results show that  $\Delta H/H_0$  decreases as the column diameter increases. As the diameter grows, the contact area between the column and the surrounding soil increases, enhancing the mobilization of lateral friction and thereby improving the column's load-bearing capacity.

#### **Effect of Geogrid Encasement**

This sub-section examines the effect of full-length geogrid encasement on the mechanical performance of sand columns. The analysis focuses on columns with (L/H=1) and varying diameters, corresponding to area replacement ratios of a = 3.5%, 7%, and 16%. Each column is fully encased along its length with a geogrid reinforcement having an axial stiffness of  $J=3000\,$  kN/m. The goal is to assess the contribution of confinement to load transfer mechanisms and the reduction of settlement.

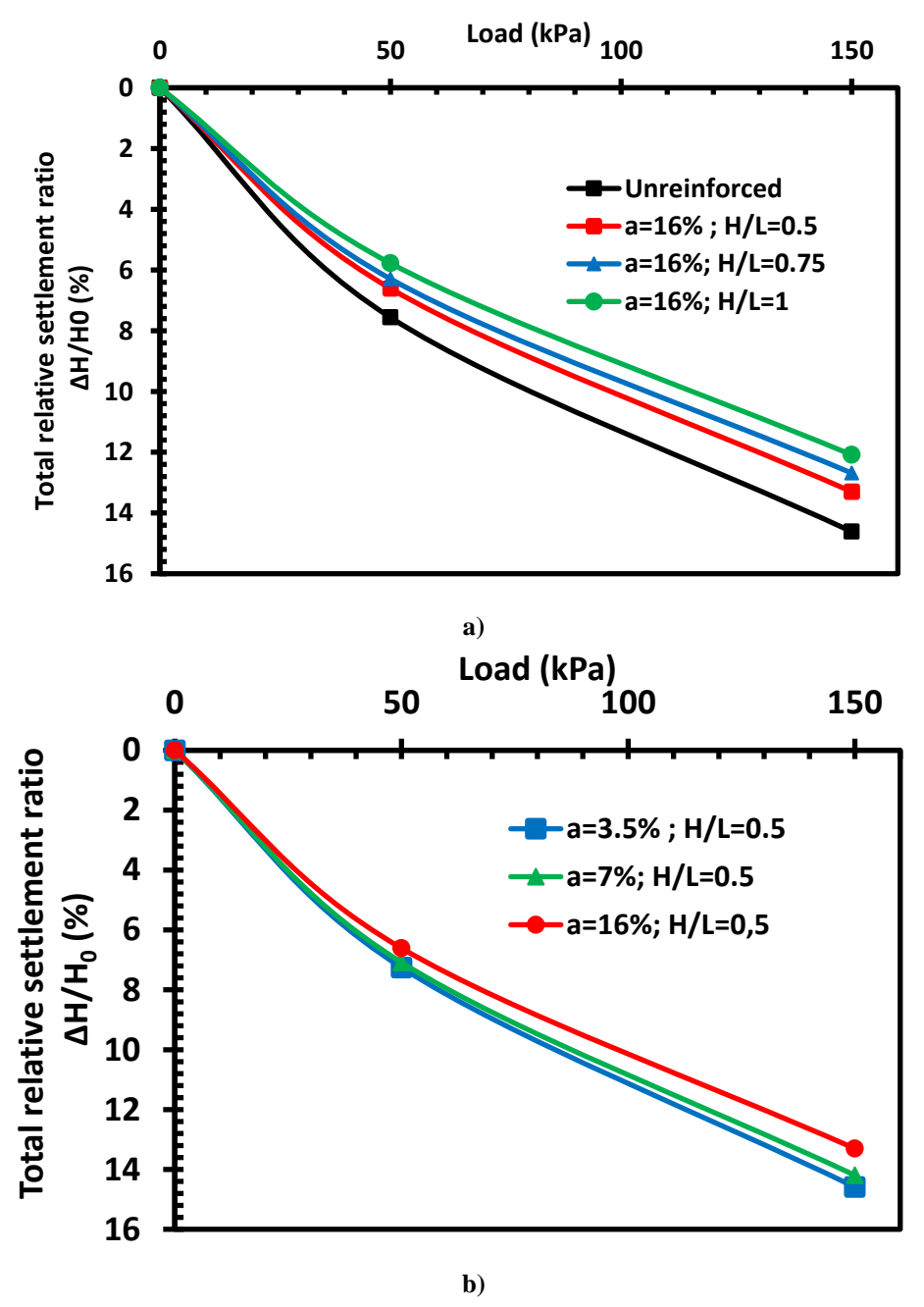


**Figure 5.** Effect of column length on total settlement: a) Effect of column length (H/L=0.5;0.75,1) for a=16%; b) Effect of area replacement ratio a for L/H=0.5

Figure 6 presents the variation in total settlement with the applied load. The results demonstrate that settlement increases with the applied load in all configurations. For area replacement ratios of 3.5%, 7%, and 16%, the total settlement values ( $\Delta H/H_0$ ) for the encased columns are 12.9%, 10.6%, and 6.9%, respectively, compared to 14.4%, 12%, and 10.6% for the columns without encasement (Figure 5a). These findings clearly illustrate the beneficial effect of geogrid encasement in reducing settlement, highlighting its role

in improving the overall performance of sand columnreinforced soils through enhanced lateral confinement.

To investigate the effect of encasement tensile stiffness on the performance of sand columns, columns with an area replacement ratio (a) of 16% and an L/H ratio of 1 were fully encased with geogrids having tensile stiffnesses of 500, 1000, and 3000 kN/m, while all other parameters were kept constant. As shown in Figure 7a, higher geogrid tensile stiffness consistently resulted in lower relative settlements under vertical

loading. Without encasement, the settlement reached 12.1% under a 150 kPa load. This was reduced to 8.4%, 7.5%, and 6.9% with increasing geogrid stiffness, demonstrating the effectiveness of geogrid encasement in enhancing ground stability. The improvement in settlement reduction primarily results from the increased confinement provided by the geogrid, which enhances the lateral stiffness of the column–soil system. As the tensile stiffness of the geogrid increases, it generates greater confining forces around the column, leading to higher axial stiffness and reduced vertical deformation. This underscores the importance of encasement stiffness

in the reinforcement of soft soils. The study also examined the effect of encasement on lateral bulging by measuring horizontal displacement along the column at different depths. Results from Figure 7b show that geogrid encasement greatly reduces lateral movement, with stiffer geogrids producing even less displacement. This indicates a clear inverse relationship between geogrid stiffness and column bulging. The added confinement limits radial expansion, thereby increasing the column's lateral stability and enhancing its overall load-bearing performance.

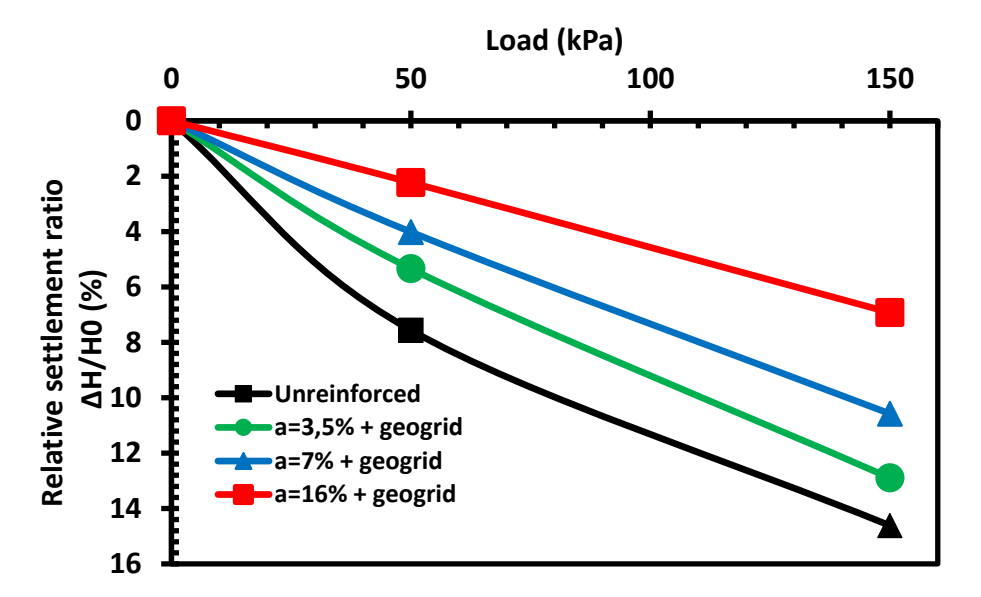
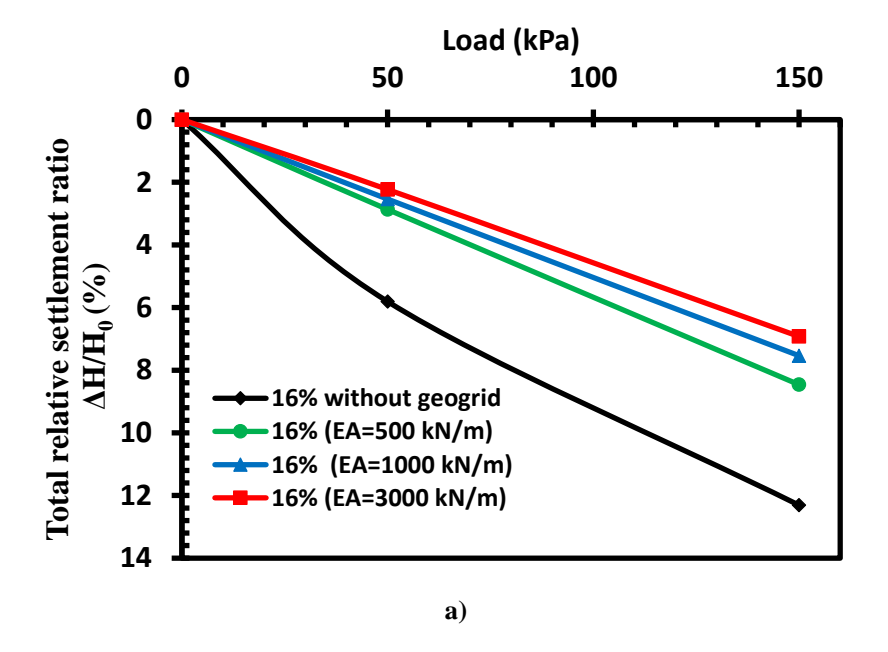


Figure 6. Effect of encasement on the total settlement (WR-NC; J = 3000 kN/m)



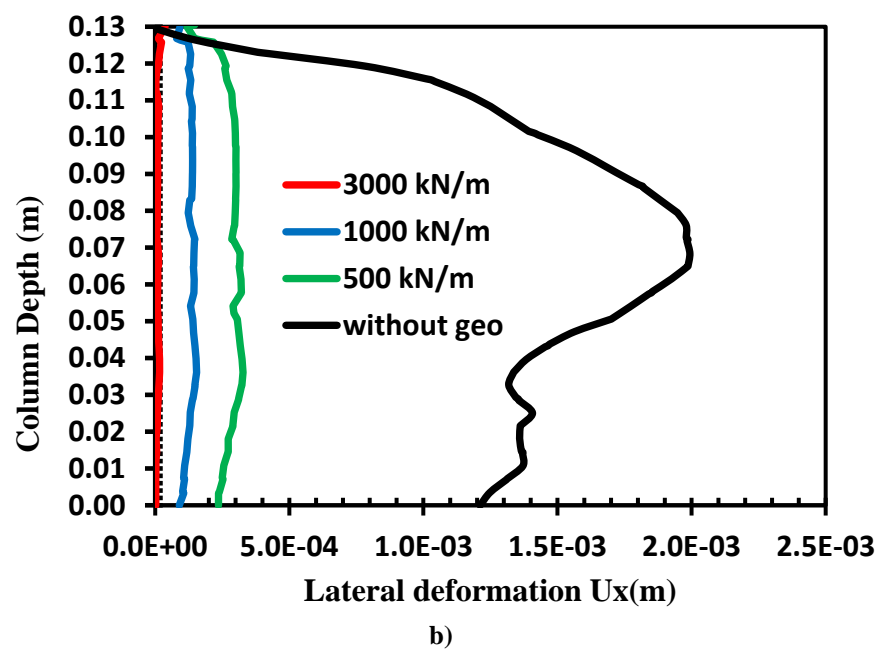


Figure 7. Effect of geogrid stiffness (WR-NC; a=16%): a) Total settlement; b) Lateral deformation

In order to evaluate the influence of geogrid stiffness on load distribution in sand column–soil systems, the Stress Concentration Ratio (SCR) is assessed. As shown in Figure 8, for a 16% area replacement ratio, SCR values increase significantly with higher geogrid stiffness. This indicates that stiffer geogrids enhance load transfer to the column, thereby reducing the stress on the surrounding soft soil and minimizing overall settlement. Specifically, SCR increases from 1.92 without encasement to 10.6, 12.7, and 15.9 with geogrid stiffness values of 500, 1000,

and 3000 kN/m, respectively.

The results presented in this sub-section highlight the beneficial effect of geogrid confinement on improving the performance of sand columns. The increase in the tensile stiffness of the geogrid enhances the confining forces around the column, reduces lateral deformation, increases axial stiffness, decreases vertical deformation, and improves load-bearing capacity. These findings underline the essential role of encasement stiffness in reinforcing soft soils and optimizing ground improvement systems.

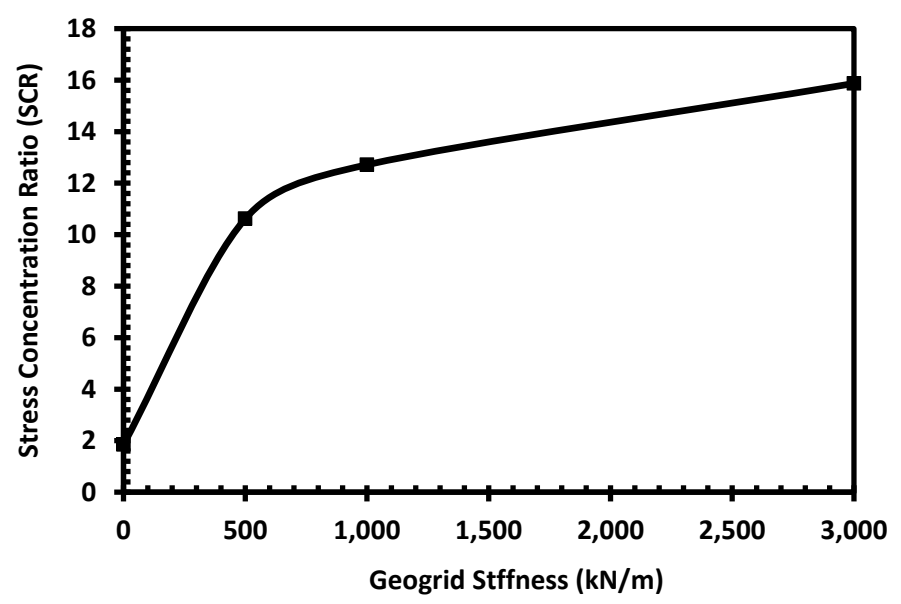


Figure 8. Stress concentration ratio as a function of geogrid stiffness (WR-NC; a=16%)

# Method with Replacement and with Compaction (WR-WC)

This sub-section evaluates the behavior of a sand column installed using the with-compaction (WR-WC) method. The column with a diameter of  $\Phi_0 = 20$  mm was constructed under three different stress levels: 73 kPa, 168 kPa, and 388 kPa. Experimental data from Phan (2010) reported relative diameter changes ( $\Delta\Phi/\Phi_0$ ) of 7%, 30%, and 77% for these stress levels, corresponding to radial expansions of 0.7 mm, 3.2 mm, and 7.7 mm, respectively. These values, representing the increase in column diameter post-compaction, were used as input parameters in numerical simulations to replicate the column's response under different compaction intensities.

#### **Effect on the Surrounding Soil**

Column installation using compaction results in radial expansion, which induces lateral soil displacement and enhances effective horizontal stress in the surrounding ground. This stress variation is expressed through the ratio  $(\sigma_{xx}'/\sigma_{x0}')$ , where  $\sigma_{xx}'$  and  $\sigma_{x0}'$  are the effective horizontal stress after and before column installation. Figure 9 presents the variation of

 $(\sigma_{xx}'/\sigma_{x0}')$  along the radial direction axis, where r is the radial distance and rc is the column radius. As compaction intensity increases, this ratio also increase. Near the column, values of 32, 35, and 40 are observed for compaction stresses of 73 kPa, 168 kPa, and 388 kPa, respectively. At greater distances from the column, these ratios reduce to 13, 16, and 22, indicating that the effect of compaction diminishes with increasing radial distance.

In addition, the radial expansion generated during column installation contributes to the densification of the adjacent soil. This effect is evidenced by a gradual reduction in the void ratio, which becomes more pronounced closer to the column. The variation of the void ratio (*e*) is quantified using the following expression:

$$\Delta e = \mathcal{E}_{v} \times (1 + e_{0}) \tag{1}$$

In this expression,  $\Delta e$  refers to the variation in void ratio, where  $e_0$  is the initial void ratio and e is the final value observed after the installation of the column. The term  $\varepsilon_{\nu}$  corresponds to the volumetric strain at the specific location under consideration.

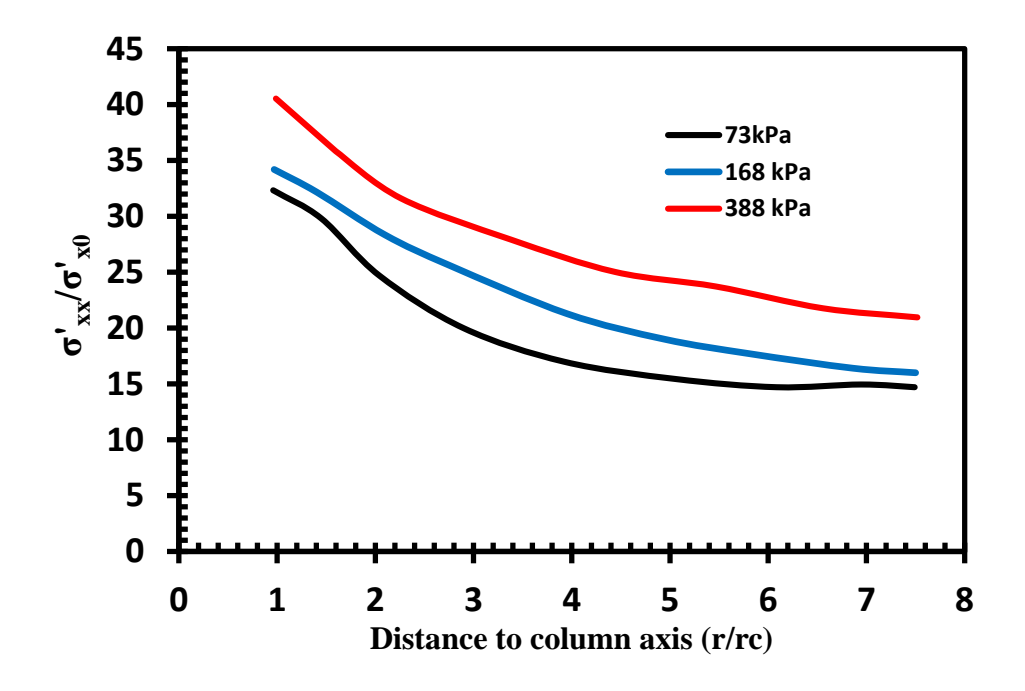


Figure 9. Effect of compaction stress on the effective horizontal stresses

Figure 10 presents the variation of the void ratio  $(\Delta e/e_0)$  with the compaction stress. The results indicate that the reduction is most pronounced in the immediate vicinity of the column and gradually becomes negligible with increasing distance. Under compaction stresses of 73 kPa, 168 kPa, and 388 kPa, the corresponding

reductions in void ratio near the column are approximately 4%, 9%, and 20%, respectively. This behavior is attributed to the radial expansion mechanism, which improves the surrounding soil by increasing effective horizontal stresses and promoting densification, particularly in areas closest to the column.

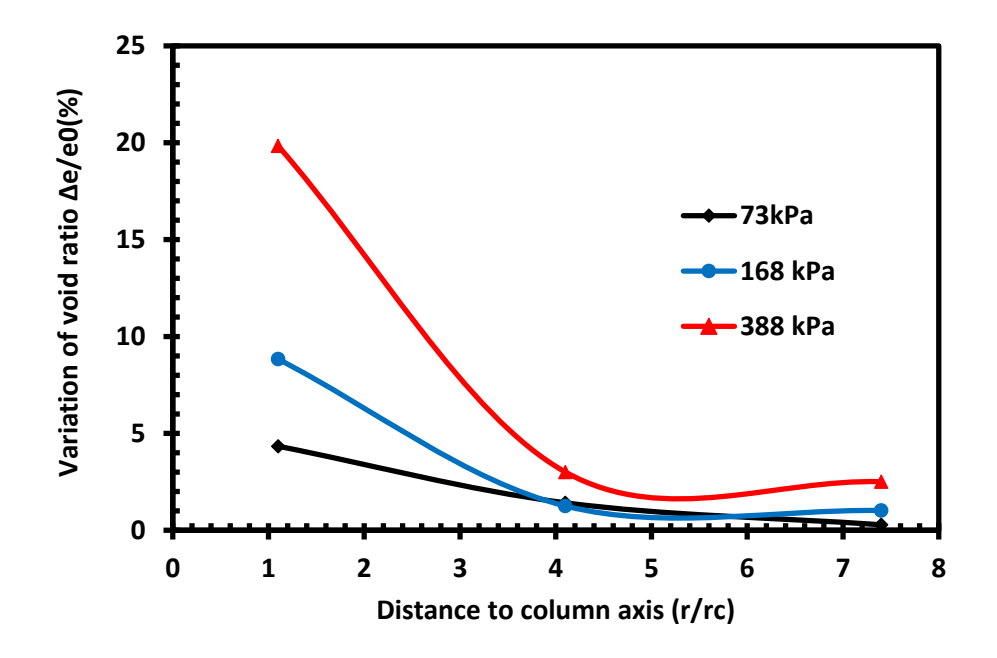


Figure 10. Effect of compaction stress on void ratio variation

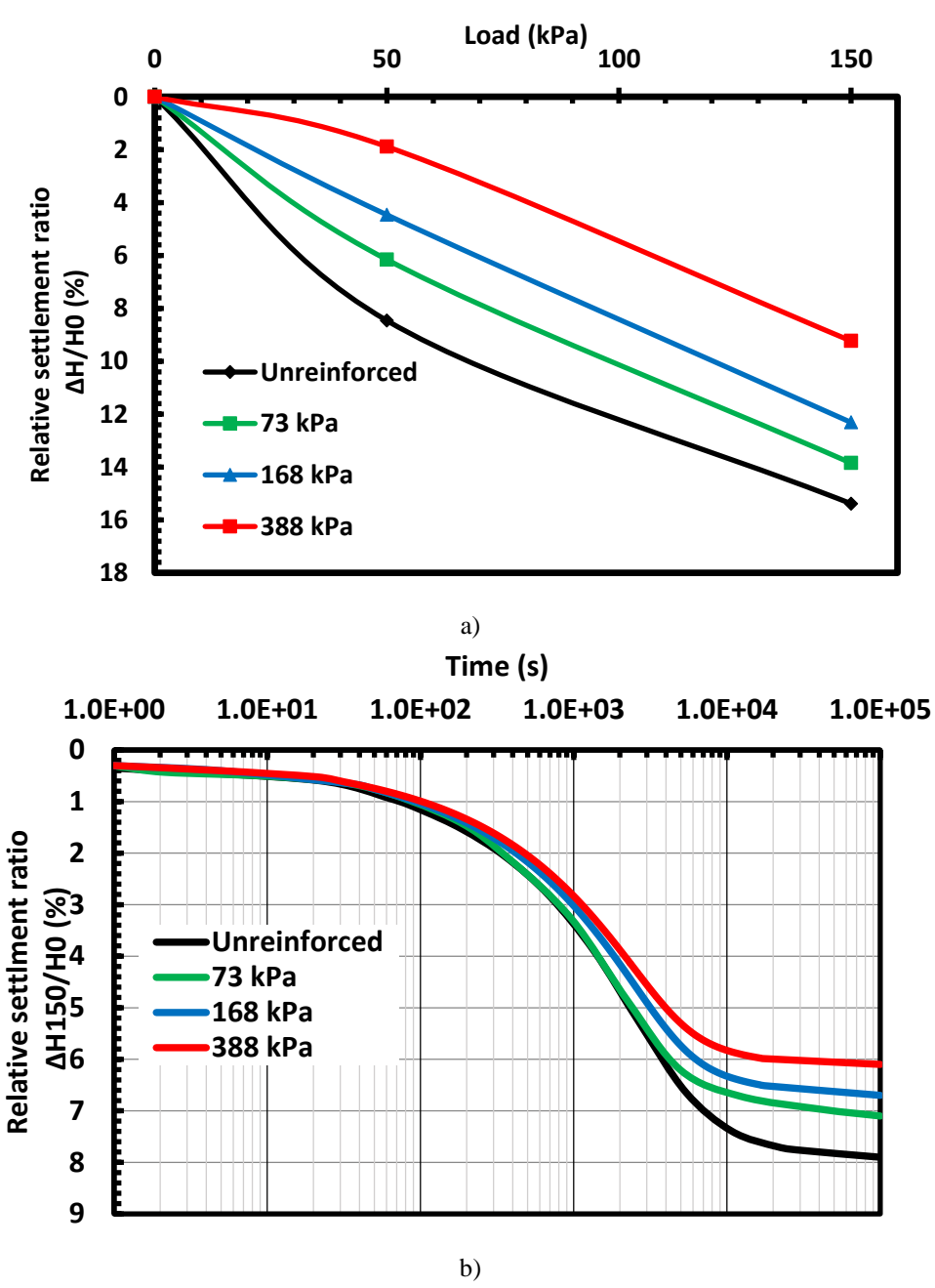
#### **Effect on the Settlement**

Figure 11a illustrates the variation in total settlement with the applied vertical load, showing a direct correlation with the loading level and an inverse relationship with the applied compaction stress. Under a loading of 150 kPa, settlements ( $\Delta H/H_0$ ) are recorded as 13.8%, 12.3%, and 9.23% for compaction stresses of 73 kPa, 168 kPa, and 388 kPa, respectively. These values correspond to settlement reductions of approximately 10%, 20%, and 40%.

The reduction in total settlement can be attributed to two primary factors: (1) the greater stiffness of the sand column relative to the surrounding native soil, and (2) the improvement in stiffness of the *in situ* soil resulting from radial expansion induced by the compaction process. Radial expansion increases the effective

horizontal stresses and reduces the void ratio in the surrounding soil, leading to soil densification and an improvement in its stiffness, and consequently, in the overall stiffness of the composite soil-column system.

Figure 11b presents the evolution of settlement (ΔH<sub>150</sub>/H<sub>0</sub>) during the consolidation phase under a load of 150 kPa. The results show a clear trend of decreasing settlement with increasing compaction stress. Specifically, relative settlements of 7.10%, 6.7%, and 6.1% were observed for stress levels of 73 kPa, 168 kPa, and 388 kPa, respectively, in comparison to 8.1% in the unreinforced (NR) condition. These reductions represent settlement improvements of approximately 10%, 15%, and 20%, respectively, demonstrating the effectiveness of compaction-induced reinforcement.



**Figure 11.** Effet of compaction stresses on settlement (WR-WC): a) Total settlement; b) Consolidation (Phase 150 kPa)

The results further demonstrate that the rate of consolidation is markedly enhanced in the reinforced case relative to the unreinforced case. This enhancement is predominantly due to the increased permeability of the sand columns, which promotes efficient pore water dissipation *via* radial drainage mechanisms.

It is also important to highlight that the consolidation rate exhibits an inverse relationship with the applied compaction stress. This behavior is explained by the densification of the surrounding soil due to radial expansion, which leads to a reduction in void ratio and, consequently, a decrease in permeability.

#### **CONCLUSIONS**

This study evaluated the performance of sand columns installed using two distinct construction techniques: with replacement without compaction (WR-NC) and with replacement with compaction (WR-WC). A parametric analysis was conducted to assess the

influence of key design parameters, including the area replacement ratio, column length, geogrid encasement, and compaction stress.

The results demonstrated that increasing the area replacement ratio significantly enhanced the load-bearing capacity of the reinforced soil. For an area replacement ratio of 16%, settlement was reduced by 17%, and the Stress Concentration Ratio (SCR) increased to 1.92. Furthermore, end-bearing columns (L/H = 1) outperformed floating columns (L/H = 0.5 and 0.75), primarily due to improved lateral friction and increased end resistance. The relative settlement decreased from 13.3% for L/H = 0.5 to 12.1% for L/H = 1.

Geogrid encasement was found to substantially improve both the load capacity and stiffness of the sand columns by providing lateral confinement, which limits radial deformation and increases internal confining pressure. The effectiveness of the geogrid was influenced by its elastic modulus. At a 16% area replacement ratio, settlement was reduced to 6.1% when a geogrid with a stiffness of 3000 kN/m was used.

The application of compaction stress during column installation further improved performance. It induced radial expansion and increased horizontal stresses, leading to a reduction of up to 20% in the void ratio of the surrounding soil. As a result, settlement decreased to 9.23% at a compaction stress of 388 kPa.

In conclusion, this study underscores the critical role of construction techniques in governing the hydromechanical behavior of soil-column systems and provides valuable insights into the optimization of reinforced ground design.

#### REFERENCES

- Aboshi, H. (1979). The composer-a method to improve characteristics of soft clay by inclusion of large diameter sand columns. *Proceedings of the International Conference on Soil Reinforcements: Reinforced Earth and Other Techniques*, 1, 211-216.
- Balaam, N.P., Brown, P.T., & Poulos, H.G. (1977). Settlement analysis of soft clays reinforced with granular piles. In *Proceedings of the 5<sup>th</sup> Southeast Asian Conference on Soil Engineering*, Bangkok, Thailand.
- Basack, S., Indraratna, B., & Rujikiatkamjorn, C. (2016). Modeling the performance of stone column–reinforced soft ground under static and cyclic loads. *Journal of Geotechnical and Geoenvironmental Engineering*, 142(2), 04015067.
- Black, J., Sivakumar, V., Madhav, M.R., & McCabe, B. (2006). An improved experimental test set-up to study the performance of granular columns. *Geotechnical Testing Journal*, 29(3), 193-199.
- Black, J., Sivakumar, V., & McKinley, J.D. (2007). Performance of clay samples reinforced with vertical granular columns. *Canadian Geotechnical Journal*, 44(1), 89-95.
- Borges, J.L. (2024). Floating stone column-supported embankments on soft soils: Numerical study incorporating stability analysis and basal reinforcement with geosynthetic. *Soils and Rocks*, 47(4),

e2024006023.

- Brinkgreve, R.B.J., Swolfs, W.M., & Engin, E. (2011). *PLAXIS 2D 2010*. PLAXIS B.V.
- Castro, J., & Karstunen, M. (2010). Numerical simulations of stone column installation. *Canadian Geotechnical Journal*, 47(10), 1127-1138.
- Cengiz, C., & Guler, E. (2020). Load bearing and settlement characteristics of geosynthetic encased columns under seismic loads. *Soil Dynamics and Earthquake Engineering*, *136*, 106244.
- Chandrawanshi, S., Kumar, R., & Jain, P.K. (2017). Settlement characteristics of soft clay reinforced with stone column: An experimental small-scale study. *International Journal of Civil Engineering Technology*, 8(5), 937-948.
- Das, M., & Dey, A.K. (2021). Improvement of bearing capacity of stone columns: An analytical study. In *Ground improvement and reinforced soil structures: Proceedings of Indian Geotechnical Conference 2020 Volume 2* (pp. 293-303). Springer Singapore.
- Ellouze, S., Bouassida, M., Bensalem, Z., & Znaidi, M.N. (2017). Numerical analysis of the installation effects on the behaviour of soft clay improved by stone columns. *Geomechanics and Geoengineering*, *12*(2), 73-85.
- El Saied, M., Abu Zeid, M., & Abdel Naiem, M.A. (2022). Numerical study of the behaviour of embankment constructed over soft soil stabilized with ordinary and geosynthetic-reinforced stone columns. *JES. Journal of*

- Engineering Sciences, 0(0), 189-204.
- Elsiragy, M. (2021). Utilization of stone column for improving seismic response of foundation on soft clay: Numerical study. *Journal of Petroleum and Mining Engineering*, 23(1), 59-64.
- Etezad, M., Hanna, A.M., & Khalifa, M. (2018). Bearing capacity of a group of stone columns in soft soil subjected to local or punching shear failures. *International Journal of Geomechanics*, 18(12), 04018169.
- Ghazavi, M., Rouhani, M., & Khoshghalb, A. (2024).
  Evaluation of the methods used for estimating the bearing capacity of stone columns. *Transportation Geotechnics*, 49, 101405.
- Gniel, J., & Bouazza, A. (2009). Improvement of soft soils using geogrid encased stone columns. *Geotextiles and Geomembranes*, 27(3), 167-175.
- Greenwood, D. A. (1970). *Mechanical improvement of soils below ground surface*. The Institution of Civil Engineers.
- Grizi, A., Al-Ani, W., & Wanatowski, D. (2022). Numerical analysis of the settlement behavior of soft soil improved with stone columns. *Applied Sciences*, 12(11), 5293.
- Guetif, Z., Bouassida, M., & Debats, J.M. (2007). Improved soft clay characteristics due to stone column installation. *Computers and Geotechnics*, 34(2), 104-111.
- Hadri, S., Messast, S., & Bekkouche, S.R. (2021).
  Numerical analysis of the performance of stone columns used for ground improvement. *Jordan Journal of Civil Engineering*, 15(2).
- Han, J., & Ye, S.L. (2001). Simplified method for consolidation rate of stone column reinforced foundations. *Journal of Geotechnical and Geoenvironmental Engineering*, 127(7), 597-603.
- Hanna, A.M., Etezad, M., & Ayadat, T. (2013). Mode of failure of a group of stone columns in soft soil. *International Journal of Geomechanics*, 13(1), 87-96.
- Hughes, J.M.O., Withers, N.J., & Greenwood, D.A. (1975).A field trial of the reinforcing effect of a stone column in soil. *Geotechnique*, 25(1), 31-44.
- Karkush, M. O., & Jabbar, A. (2019). Improvement of soft soil using linear distributed floating stone columns under foundation subjected to static and cyclic loading. *Civil Engineering Journal*, 5(3), 702-711. <a href="https://doi.org/10.28991/cej-2019-03091264">https://doi.org/10.28991/cej-2019-03091264</a>
- Karkush, M., & Jabbar, A. (2022a). Behavior of floating

- stone columns and development of porewater pressure under cyclic loading. *Transportation Infrastructure Geotechnology*, 9(2), 236-249.
- Karkush, M., & Jabbar, A. (2022b). Effect of several patterns of floating stone columns on the bearing capacity and porewater pressure in saturated soft soil. *Journal of Engineering Research*, 10(2B), 84-97.
- Karkush, M.O., Jihad, A.G., Jawad, K.A., Ali, M.S., & Noman, B. J. (2021). Seismic analysis of floating stone columns in soft clayey soil. In *E3S Web of Conferences* (Vol. 318, p. 01008). EDP Sciences.
- Laouche, M., Karech, T., Rangeard, D., & Martinez, J. (2021). Experimental study of the effects of installation of sand columns in compressible clay using a reduced model. *Geotechnical and Geological Engineering*, 39, 2301-2312.
- Madahv, M.R. (2006). Engineering of ground by stone columns/granular piles. In *Proceedings of the ATC-7 Workshop on Stone Column in Soft Deposits* (pp. 1-17). Busan, Korea.
- Murugesan, S., & Rajagopal, K. (2006). Geosyntheticencased stone columns: Numerical evaluation. *Geotextiles and Geomembranes*, 24(6), 349-358.
- Phan, V.T.P. (2010). Renforcement des sols compressibles par colonnes ballastées (Doctoral dissertation, National Institute of Applied Sciences, Rennes, France).
- Priebe, H. (1976). Estimating settlements in a gravel column consolidated soil. *Die Bautechnik*, 53, 160-162.
- Priebe, H.J. (1995). The design of vibro replacement. *Ground Engineering*, 28(10), 31.
- Poorooshasb, H. B., & Meyerhof, G.G. (1996). Consolidation settlement of rafts supported by stone columns. *Geotechnical Engineering*, 27, 83-92.
- Rashwan, S.I., Nasr, A.M., & Azzam, W.R. (2025).
  Numerical analysis considering the dynamic installation effects of stone column on soft clay response. *Jordan Journal of Civil Engineering*, 19(3).
- Sivakumar, V., McKelvey, D., Graham, J., & Hughes, D. (2004). Triaxial tests on model sand columns in clay. *Canadian Geotechnical Journal*, *41*(2), 299-312.
- Tai, P., Indraratna, B., Rujikiatkamjorn, C., Chen, R., & Li, Z. (2024). Cyclic behaviour of stone column reinforced subgrade under partially drained condition. *Transportation Geotechnics*, 47, 101281.
- Tan, X., Feng, L., Hu, Z., & Zhao, M. (2021). Failure modes and ultimate bearing capacity of the isolated stone column in soft soil. *Bulletin of Engineering*

Geology and the Environment, 80(3), 2629-2642.Yoo, C. (2010). Performance of geosynthetic-encased stone columns in embankment construction: Numerical investigation. Journal of Geotechnical and

Geoenvironmental Engineering, 136(8), 1148-1160.Yoo, C., & Kim, S.B. (2009). Numerical modeling of geosynthetic-encased stone column-reinforced ground.Geosynthetics International, 16(3), 116-126.